5-2017

Modeling De Novo Granulation of Anaerobic Sludge

Honey Varghese
Utah State University

MODELING DE NOVO GRANULATION OF ANAEROBIC SLUDGE

by

Honey Varghese

A thesis submitted in partial fulfillment
of the requirements for the degree

of

MASTER OF SCIENCE

in

Computer Science

Approved:

Nicholas S. Flann, Ph.D. Major Professor	Vladimir Kulyukin, Ph.D. Committee Member
Vicki Allan, Ph.D. Committee Member	Mark R. McLellan, Ph.D. Vice President for Research and Dean of the School of Graduate Studies

UTAH STATE UNIVERSITY
Logan, Utah

2017

ABSTRACT

Modeling De Novo Granulation of Anaerobic Sludge

by

Honey Varghese, Master of Science

Utah State University, 2017

Major Professor: Nicholas S. Flann, Ph.D.
Department: Computer Science

The enigma of anaerobic sludge granulation is still exciting the minds of both experimental scientists and modeling experts. A unique combination of mechanical, physiochemical and biological forces influence granulation during processes of anaerobic digestion. However, knowledge of potential driving forces of granulation has not been transformed into a comprehensive model of anaerobic granulation. In this computational experiment, we address the role physiochemical and biological processes play in granulation and provide a literature-validated working model of anaerobic granule de novo formation. The model developed in a cDynoMiCs simulation environment successfully demonstrated a de novo granulation in a glucose fed system. The simulated granules exhibit experimental observations of radial stratification: a central dead core surrounded by methanogens then encased in acidogens. Practical application of the granulation model was assessed on the anaerobic digestion of low-strength wastewater by measuring the changes in methane yield as model parameters were systematically swept. This model will be expanded in the future to investigate the influence of mechanical forces on the de novo granulation and the application of a model to anaerobic digestion of a complex protein-carbohydrate rich feedstock.

(52 pages)

PUBLIC ABSTRACT

Modeling De Novo Granulation of Anaerobic Sludge

Honey Varghese

The global market for biological waste water treatment is large and growing. Bio-engineered reactor setups employ microorganisms to degrade waste and produce useful/less harmful components. Scientists are interested in studies that reveal the biological mechanisms involved in the process of these microbial actions in order to improve the reactor performance. The process of granulation in aerobic sludge is one such interesting process which is less explained.

The primary goal of the thesis is to design a computational model that simulates the process of granulation in anaerobic sludge and that addresses the role physiochemical and biological processes play in granule formation. The working model that we have developed has been validated using the existing literature. The model successfully demonstrates granulation in a glucose fed system with formation of 0.5 mm mature granule in 33 days with the production of methane. The simulated granules have the same structure as that of the real world granule images: a central dead core surrounded by living cells (acidogens and methanogens).

The model can also be used by scientists as a tool to find the parameter values that can help in tuning the reactor to maximize productivity. As an application of the tool, we have built a search engine that systematically sweeps the model parameters to find the amount of food supply (glucose) and the ratio of different microbe species in initial feed to the reactor. The model can also be expanded in the future to investigate more complex processes.

ACKNOWLEDGMENTS

I would like to express the deepest appreciation to my committee chair, Dr. Nicholas Flann. Without his guidance and persistent help this dissertation would not have been possible.

I would like to thank all my committee members for their continued support. In addition, thanks to my co-author Anna Doloman who helped in making this work biologically realistic and to my friend Delin Davis who supported me in every step of this work.

Honey Varghese

CONTENTS

Page

ABSTRACT iii

PUBLIC ABSTRACT iv

ACKNOWLEDGMENTS v

LIST OF TABLES vii

LIST OF FIGURES viii

ACRONYMS ix

CHAPTER

1 INTRODUCTION 1

2 MODEL EXPERIMENT AND MODEL 4

3 RESULTS 5
- 3.0.1 Study I: Reactor scale model 5
- 3.0.2 Study IIa: Stages of granule formation 6
- 3.0.3 Study IIb: Analysis of granule growth dynamics 9
- 3.0.4 Study III: Formation of a mature granule 11
- 3.0.5 Validation of the model 12
- 3.0.6 Parameter scan for optimized methane production 14

4 METHODS 17

5 DISCUSSION AND CONCLUSIONS 22

REFERENCES 24

APPENDICES 29
- A Protocol file for the model 30
  - A.1 Description 30
  - A.2 Protocol file 30

LIST OF TABLES

Table Page

4.1 Parameters used in model and their literature values 19

LIST OF FIGURES

Figure		Page
3.1	Reactor scale model.	6
3.2	Stages of simulated *de novo* granulation and associated dynamic changes in the solutes concentrations	8
3.3	A close-up of the dynamic changes	10
3.4	Validation of the *de novo* granulation model via qualitative analysis.	12
3.5	Validation of the *de novo* granulation model via quantitative analysis.	14
3.6	Parameter scan for the methane production in simulated granule	15

ACRONYMS

pH	Potential of Hydrogen
μm	Micrometers
mg	Milligrams
mm	Millimeters
g/L	Gram per Liter
AD	Anaerobic Digestion
UASB	Up-flow Anaerobic Sludge Blanket Reactor
ECP	Extracellular Polymer
ADM	Anaerobic Digestion Model

CHAPTER 1

INTRODUCTION

An efficient anaerobic digestion (AD) of organic matter is a result of a complex microbial interaction inside a bioreactor. For the high-rate anaerobic digestion of a feedstock, an up-flow anaerobic sludge blanket reactor (UASB) is a common choice. The superior performance of this reactor is due to the particular organization of microorganisms into spherical granular structures. The process of granulation was first noticed and documented in the early 1980s [1, 2] and since then a number of anaerobic granulation theories have been presented. The main reasoning for the granulation *per se* is the up-flow velocity inside sludge bed of a UASB reactor. Microbial cells moving up with the flow of the feed tend to stick to the other microbial cells. Such sticking behavior prevents a washout of the microbial inoculum from a reactor since the outlet for the digested feed is located in the top of the reactor [3,4]. The most widely accepted theory states that granulation starts with a formation of a future granules core, comprised of filamentous methanogenic bacteria *Methanothrix*, together with *Methanosarcina*, which secrete extracellular polymers (ECP) [5–7]. The surface of this changes and become attractive for the oppositely charged anaerobic bacteria that are present in the dispersed inoculum of a UASB rector [8–10]. Chemo-attractance of other bacteria towards ECPs and substrate around the granule core may also play a major role in the further aggregation and formation of mature granules [11, 12]. Despite these possible explanations of the granulation process, there is still no agreement on which of the possible theories correctly explain this most important and crucial role of granulation. The key factors of granulation are still to be determined, whether they are physical, biochemical or a combination of physicochemical properties of the cells and the way the organic matter transforms over space and time.

An effective means to get a better understanding the granulation process is through the construction of a computational granulation model. This model must incorporate testing of different key granulation factors. There are already some granulation models available in the literature, but they do not describe a process of *de novo* granulation and only describe

the kinetics of anaerobic digestion with an already mature granular consortia. For example, one of the earliest models by Tartakovsky and Guiot [13] assumes a layered granule structure with a homogeneous distribution of microbial groups from the very beginning of the simulation. Authors describe the kinetics of substrate transformation in a mature granule that reached a steady state. Using the same assumption, Arcand et al. [14] successfully predicted the substrate distribution inside a granule, based on diffusivity gradient inside a biomass. Shayegan et al. [15] took the substrate kinetics in the granule one step further, incorporating behavior of granular agglomerates into the operation predictions of the whole UASB reactor. The mass of granules in a reactor, rates of granule decline and general bacterial growth kinetics were used as a basis for the model. Skiadas and Ahring [16] have applied a cellular automata theory, developed by Wimpenny et al. [17], to model granulation during anaerobic digestion. However, authors assumed a homogeneous layered structure of a granule and obtained calculated values of substrate utilization rates that do not agree with the experimental data they used as a reference.

A commonly applied assumption of a homogenous-layered structure of anaerobic granule does not conform with experimental data. In particular, data suggests a spatially organized granule containing a mixed composition of bacterial groups inside the granule. In models lacking this property, there is no strict compartmentalization of trophic groups, like methanogens and acidogens, in the core and outer layer, respectively. Strict anaerobes, like methanogens, can also be found in the outer layer of the granule, as visualized with fluorescent probing experiments and scanning electron microscopy [18–21]. A non-homogeneous bacterial distribution is investigated in a model described by Picioreanu et al. [22]. However, the study does not address the process of granulation itself, and an entirely formed granule is employed as an initial condition and seed of a model. The model, therefore, predicts a mature granule's further development, growth, and formation of an inside inert core.

An enormous amount of knowledge has been developed concerning predicting the rates of anaerobic digestion in UASB reactors with mature granules. However, these models are not complete and do not represent the actual input for large scale applications, specifically

those of the widely accepted biochemical model of the anaerobic digestion process (ADM1) [23]. The most recent review of the current status of ADM1 clearly states the need to thoroughly address the application of ADM1 to various types of anaerobic reactors, UASB in particular. Thus, a complete and trustful model of anaerobic digestion in UASB must take into account both granulation in general and initial *de novo* granulation [24]. Knowledge of the critical parameters facilitating *de novo* granule formation will aid in robust UASB reactor operation and production of increased methane yields with high organic matter transformation rates.

A model of *de novo* granulation proposed in this paper addresses some of the key aspects that influence aggregation of microbial biomass into defined granular structures. Those key elements include: initial concentrations of the substrate used as a feedstock for anaerobic digestion; ratio of methanogenic and acidogenic cells at the start of the reactor; the role of chemotactic attractions and cell-to-cell adhesion properties. This study addresses all these factors. Additionally, an extensive computational search of the initial parameter values is made to determine an optimal initial combination that yields the highest start-up methane production rates.

CHAPTER 2

MODEL EXPERIMENT AND MODEL

The process of granulation is modeled at two spatial scales in the simulation. At the macro scale, the reactor process is simulated where the cells are introduced into an agitated system (due to the upflow velocity in UASB reactor), cells interact and form multiple agglomerates (centers of granulation). At the mesoscale, simulations are performed that focus on the growth and development of one such agglomerate into a mature granule.

In the macro scale, randomly distributed acidogenic (further referred to as "acidogens") and methanogenic cells (further referred to as "methanogens") are introduced into random positions within the reactor. The particles experience mechanical forces due to agitation in the system as well as biomechanical forces due to homogeneous and heterogeneous adhesion and formation of EPS-driven interactions. As a cumulative effect of these forces, cells come close to each other and form several agglomerates.

To closely monitor the growth patterns in the formation of a granule, the mesoscale simulation is designed to focus on the development of a single granule (from the initial agglomerate of acidogens and methanogens formed during the macro studies). In UASB bioreactors, granules move freely in an agitated system, where the supplied solutes are relatively mixed. To simulate such a mixed environment for the granule growth, we provide a continuous supply of one solute (glucose) from all the sides of the simulation domain with diffusivity as defined in Table 4.1 . The model executes growth reactions that represent the consumption of the supplied glucose by the acidogens, the secretion of the acetate as a metabolite of acidogens and the consumption of acetate by methanogens, which is converted into the methane gas.

CHAPTER 3

RESULTS

Simulation experiments were conducted on the computational granulation model to give insights into different stages in the development of granules in aerobic sludge reactors. Where available, literature supported model parameters [listed in Table 4.1] were employed. Other parameters, such as those that influence particle aggregation and mechanical sorting, were fine-tuned based on correspondence between observations made from simulations and comparisons with reported granule images. The resulting granule spatial organization and product production of model simulations were analyzed and compared with values from real biological systems. Another objective of the study was to employ a search engine to find the amount of initial glucose concentration and populations of methanogens and acidogens that lead to optimal methane production.

3.0.1 Study I: Reactor scale model

In the Phase I of modeling, randomly distributed acidogens and methanogens (illustrated in Figure 3.1a) interact with each other in a simulated UASB reactor environment, where upflow velocity and agitation play key roles to promote granulation of sludge. In the simulated environment microbial cells move around the system due to agitation and cells are bound together due to biomechanical adhesive forces, allowing formation of cell agglomerates (illustrated in Figure 3.1b).

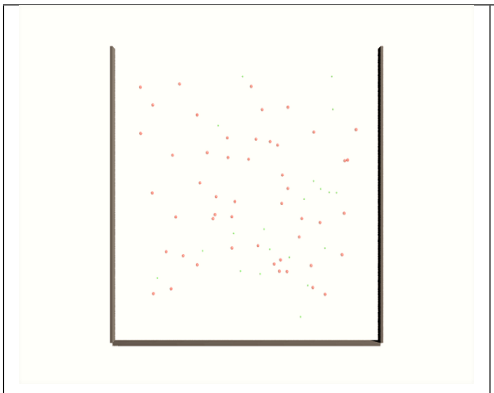

Initial random distribution of two types of cells in a UASB-like environment.

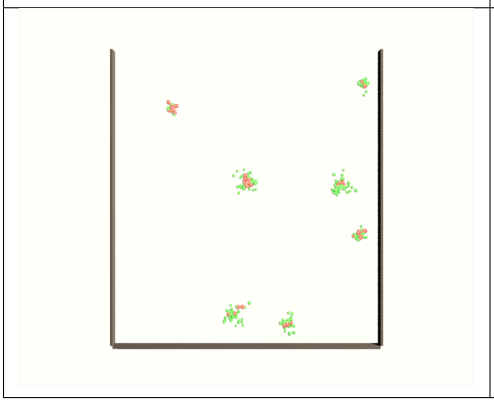

Cells self-organize into a cluster due to the mechanical forces caused by agitation in the system and mutual adhesion between two cell types.

Fig. 3.1: Reactor scale model.
a) initial random distribution of two types of cells in a UASB-like environment; b) formation of cell aggregates due to the mechanical forces, mutual adhesion and random agitation in the UASB-like environment.

3.0.2 Study IIa: Stages of granule formation

To investigate the development of a mature granule and dynamic changes in the cell growth, consumption of glucose, a series of simulator output snapshots were performed (Figure 3.2). At the initial stage (t=0 hours), single cell aggregate appear as a small cluster of acidogens and methanogens (zoomed from Phase I Reactor scale model, Figure 3.1). As time proceeds (t=300, t=480 and t=700 hours) cells grow and corresponding solute gradients demonstrate accumulation of acetate and methane in the system. Methane, being a volatile compound, is slowly diffused out of the system and depicted values on the scale of gradient images are not the cumulative values, as in the case of the glucose and acetate. At 480 hours of granule development, a black “dead” core of cells start to emerge in the middle of the granule sphere. Appearance of a “dead” core is due to the diffusion boundaries

of glucose or acetate inside granular cluster. Thus, cells of both types (acidogens and methanogens) are not getting enough energy supply and are forced to transition into the inert biomass. This transition is set to be irreversible in the model, thus leading to a formation of a "dead core". A similar core can be seen on the Figure 4a of the laboratory-observed granule, which is used as evaluation criterion in current study and is described later in detail. The final stage of granule development simulation (t=650 hours) demonstrates a mature granule with 0.5 mm in diameter.

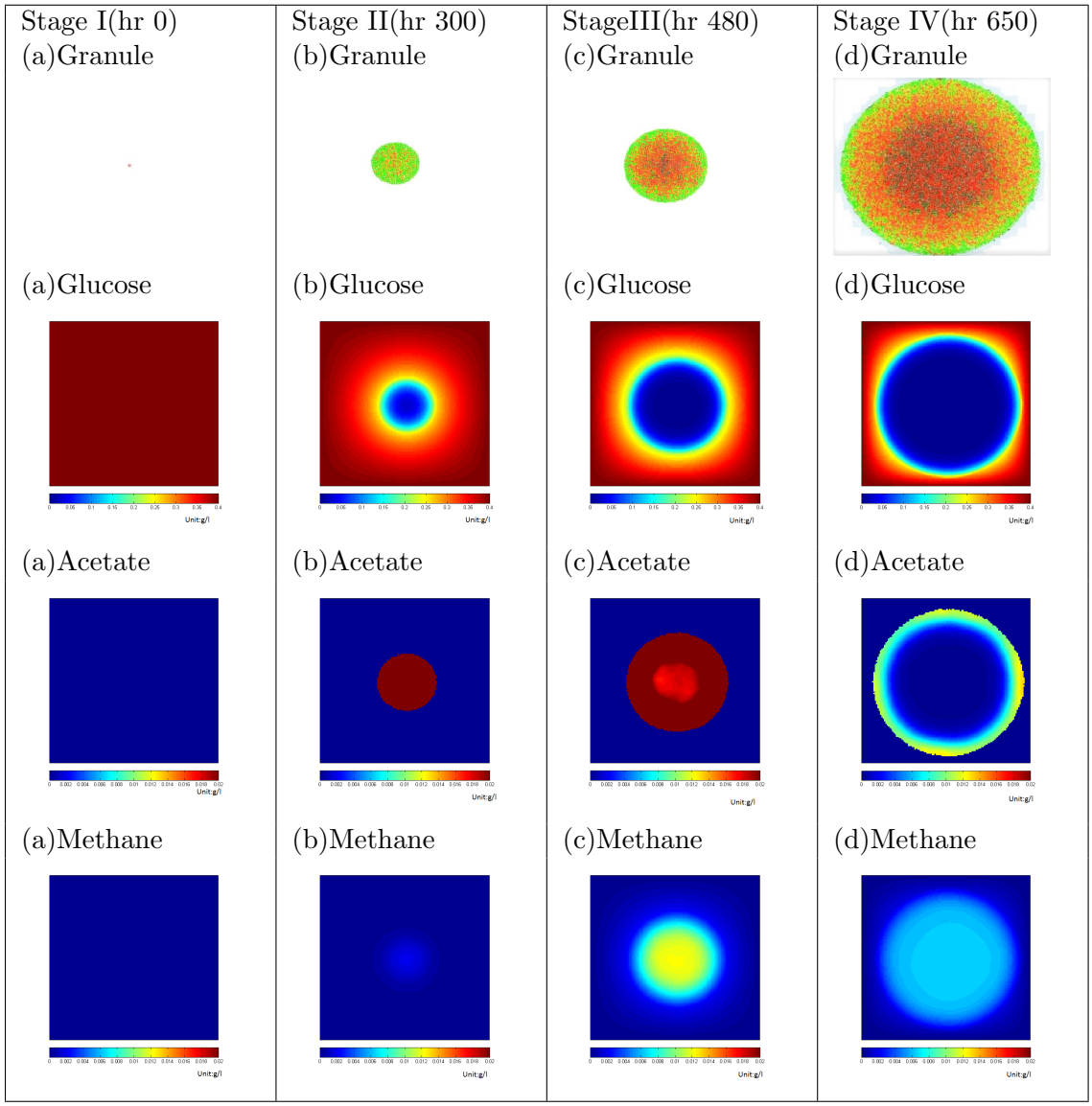

Fig. 3.2: Stages of simulated *de novo* granulation and associated dynamic changes in the solutes concentrations

3.0.3 Study IIb: Analysis of granule growth dynamics

In addition to visual (qualitative) investigation of *de novo* granulation, a close up quantitative study was performed on dynamic changes in solute amounts and cell biomass accumulation (both in values of cell numbers and cell biomass numbers). Graphs for dynamic changes are provided in Figure 3.3. Figure 3.3a demonstrates changes in the total number of two types of cells (acidogens and methanogens) with regard to the simulation time. Simulation was initiated with 100 cells of each type. Due to the fast growth of the acidogens (see the Table1 with growth kinetics parameters), we can see an exponential growth of acidogens from t=80h to t=360. A similar dynamic is depicted in Figure 3.3 b. Due to the product inhibition by the produced acetate and lack of diffused glucose, acidogens decrease their relative growth rate and reach the stationary phase of growth at around t=600h.

Dynamics of methanogens growth is slightly different, mainly due to the lack of available acetate from the start-up of the system and a lower growth rate, contrary to acidogens (Table 1 with model parameters). Methanogen growth goes through a long lag phase (t=0h until t=220h), where biomass is accumulated at a very slow rate (Figure 3.3 c). At this lag phase methanogen cells are waiting for the supply of acetate from acidogens. As soon as enough acetate is accumulated in the system (around t=220h), methanogens start exponential growth and decrease their relative growth rate at about t=520h. This decrease is in direct correspondence with the amount of available acetate in the system at the same time period (t=480-500h), when acidogens are inhibited by the produced acetate and are not provided with a high flow of glucose (due to the slow diffusion into the center of the granular biomass). Kinetics of acetate accumulation/conversion and methane production are in a good correlation with experimental data reported by Kalyzhnyy et al. and others [25–28]

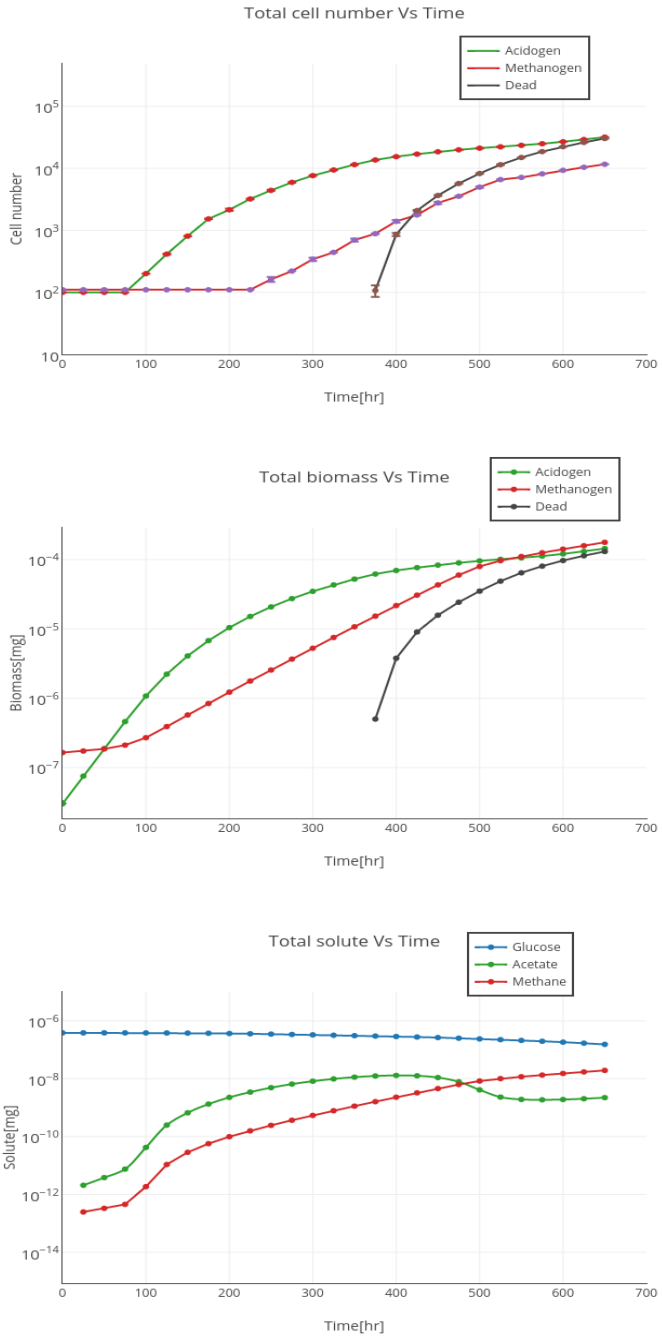

Fig. 3.3: A close-up of the dynamic changes
a) Total cell number over simulation time, b) Total cell biomass over simulation time and c) Total solute concentration over simulation time. All the changes are graphed for each type of the cell (acidogens, methanogens, inert dead type) and each type of the solute (glucose, acetate, methane). 10 simulations with different random seeds were graphed to demonstrate standard deviation in the monitored values.

3.0.4 Study III: Formation of a mature granule

Figure 4 shows images of a 1mm in diameter granule, obtained from both a laboratory experiment reported by Sekiguchi et al. [19] (Figure 3.4a) and an image from our simulated model (Figure 3.4b). Simulation of 1mm in diameter granule formation took 800 hours (around 33 days), which corresponds to the published studies observing granulation in UASB reactors [20,29]. Images 4c, 4d and 4e depict distribution of solutes (glucose, acetate, and methane) at the final stage of simulated granule growth (t=800 hours). One can note a sharp decrease in the glucose diffusion inside the granule, with regard to the biofilm diffusivity capacity. Since acetate is consumed by methanogens during their growth and converted to methane, there is a low concentration gradient of both chemicals on the final images (Figure 3.4c,d,e).

Overall, solute distributions for 1mm granule follow a similar pattern as for the 0.5mm granule, described earlier. Key point in conducting simulation of a 1mm granule development is to demonstrate radial growth, without substantial changes in the overall morphology. Thus, initial stages of granule formation (Phase I) are the key factors for granulation *per se*.

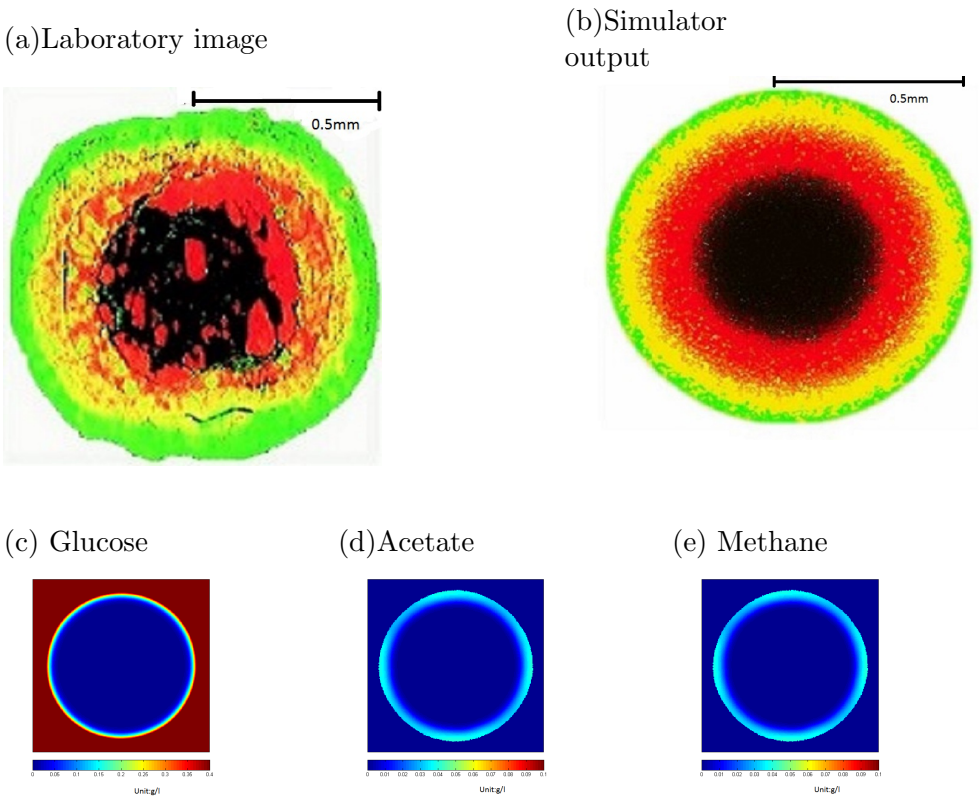

Fig. 3.4: Validation of the *de novo* granulation model via qualitative analysis. a) Laboratory image courtesy of [19]. b) An image of granule simulated with current model. c) Distribution of the three solutes defining simulation of granulation (glucose, acetate, methane) at the final time point (t=800 hours) of the simulation.

3.0.5 Validation of the model

Validation of the model performance was conducted both qualitatively and quantitatively (Figure 3.5). Visual comparison of a published fluorescent-labeled image of granule with simulated granule image demonstrates a striking similarity in spatial distribution of main trophic groups of microorganisms - acidogens, methanogens and "dead" biomass.

Irregularities and hollow parts (black color) in the published granule image (Figure 3.4a) are possibly caused by the upflow velocity of the liquid and particulate matter in a UASB reactor, where the granule was developed [19], which might have damaged spherical shape of the immature granule, causing mature granule to change its shape and grow further with hollow compartments. Another possible explanation might be granule division. It is

well documented [8–10] that due to the shear stress in a UASB reactor, granules cannot grow uncontrollably and will eventually split into “daughter granules. Those “daughter granules are susceptible to attachments of additional microbial cells, floating in UASB sludge bed. Those newly attached cells might cause irregularities in future mature granules in forms of randomly distributed cell clusters in a presumably inert (“dead) core (red-labeled cell clusters on Figure 3.5a).

To validate our simulated model quantitatively, we conducted image processing of the published data and used an algorithm to count the number of distinctly colored pixels/cells at the different distances from the center of the granule image (Figure 3.5). We used 4 quarters of a spherical granule in the analysis to provide standard deviations of spatial distribution of three distinct cell groups acidogens, methanogens and inert (dead) biomass. Results of quantitative distribution of three main cell types in both simulated and real images are in a good correlation, accept for the radial section 3. Such slight discrepancy is due to the possible “division to daughter granules history of the laboratory granule.

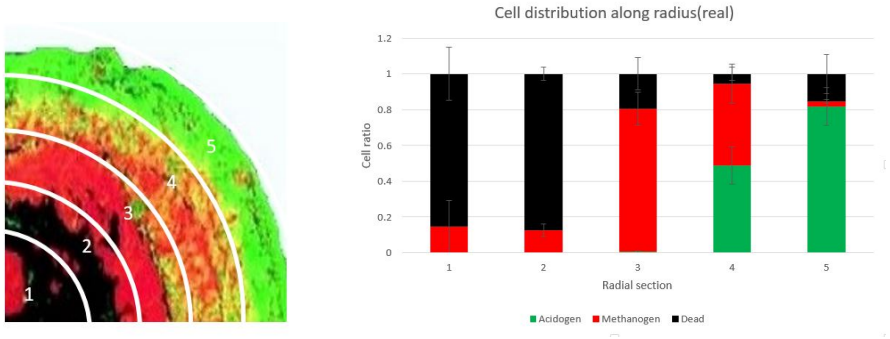

(a) Laboratory

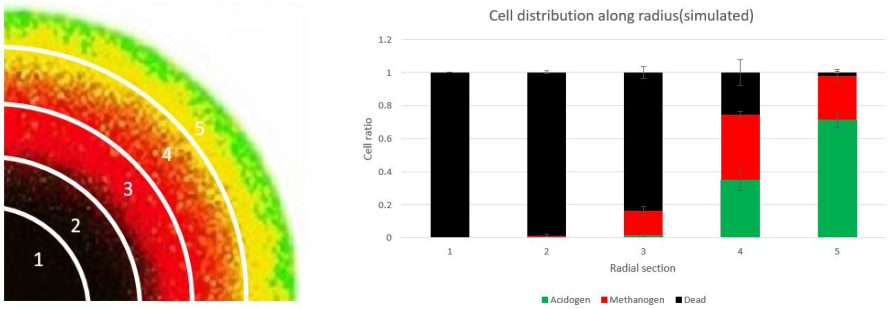

(c) Simulated

Fig. 3.5: Validation of the *de novo* granulation model via quantitative analysis. Validation was done via analysis of the three cell type radial distribution in the both laboratory and simulated granule. Both granules were divided into four quarters and each quarter was analyzed for cell distribution. Differences in the cell numbers at the same radial distance in four quarters are depicted in a form of standard deviation. Red, green and black colors of the bars on bar chart represent acidogen, methanogen and dead cells respectively.

3.0.6 Parameter scan for optimized methane production

Main objective of the parameter scan is to estimate a combination of cell ratio (acidogens:methanogens) and glucose supply needed to start anaerobic system to achieve a desired (maximum) methane yield. The corresponding protocol parameter for glucose value is “SBulk” in world section. The “init area number” for acidogens and methanogens in the species section is used to determine the initial cell ratio for the simulations. The minimum and maximum value of the interval in which the search should be performed is given as an input to the search engine. The methane productivity (calculated from the solute concen-

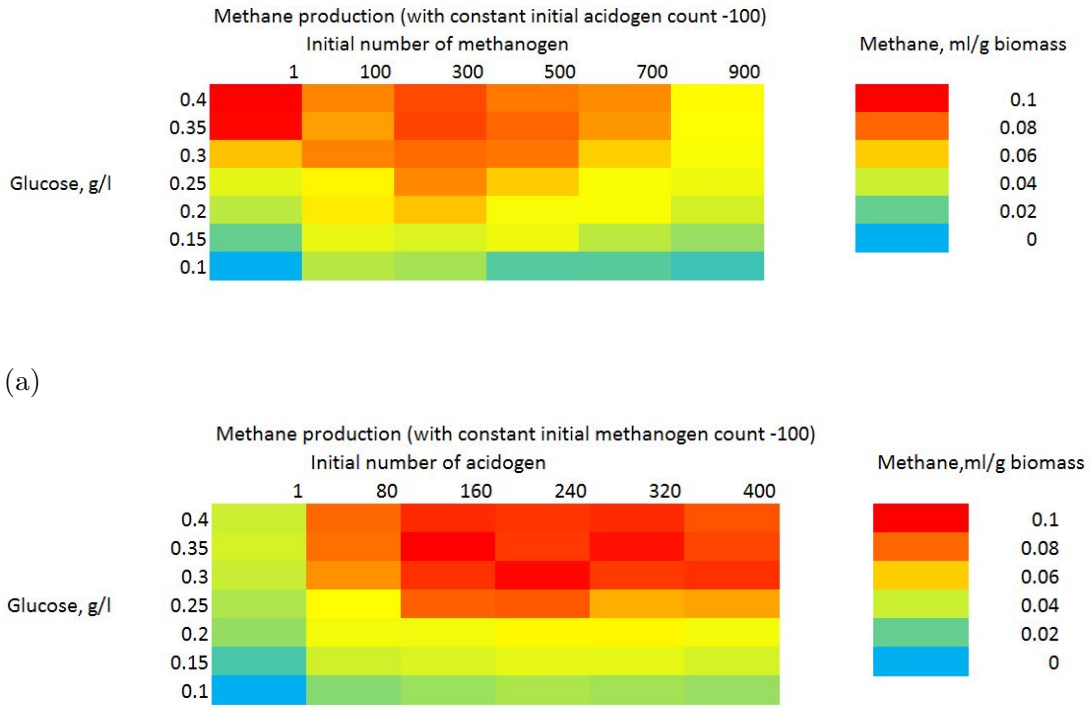

Fig. 3.6: Parameter scan for the methane production in simulated granule a) Varying initial number of methanogen cells (constant initial acidogen cell count) and b) Varying initial number of acidogen cells (constant initial methanogen cell count). Red color of the heatmap section has the highest value of methane produced (in milliliters of methane per gram of biomass), while blue heatmap section has the lowest value of produced methane. Parameter scan was conducted for 0.5mm granule size and for the period of 650 simulation hours.

tration file output from simulator) is given as fitness function for the engine. The search engine simulated granule formation for several combinations of parameter values within the input interval and calculated total methane produced. The result is produced as a heatmap in Figure 3.6.

Figure 6 depicts amount of methane produced (in milliliters) per gram of biomass with varying amount of glucose supplied initially into the system (0.1 to 0.4 g/l). Figure 3.6a has a constant initial acidogen count of 100 cells, and heatmap demonstrates varying amounts of methane produced with different glucose concentrations and different numbers of initial

methanogen cells (from 1 to 900 cells). Same scheme is followed on Figure 3.6b, but with varying initial numbers of acidogens (from 1 to 400) and constant initial methanogen count of 100 cells.

One can note from both Figure 3.6a and Figure 3.6b that increased amount of glucose correlates with increased amount of methane produced in the system. Also, in general increased number of starting cells of acidogens (Figure 3.6b) let to the higher amounts of methane produced. This correlates with the earlier explored kinetics of methanogen/acidogen growth, when methanogens are waiting for acetate supply until they start to grow and produce methane.

Parameter scan also helped to identify an important observation that a ratio of methanogen cells to acidogens should not be in a high favor of methanogens (100 acidogens and 900 methanogens on Figure 3.6a), since this leads to a decreased amount of methane production. The reason for such correlation is lack of acetate in the system to support growth of such a big number of methanogenic cells, which are forced to starve and die off.

CHAPTER 4

METHODS

An agent-based simulator framework, *cDynoMiCs* [30] is used in this experiment. *cDynoMiCs* is an extension of *iDynoMiCs* framework developed by the Kreft group at University of Birmingham [31] specifically for modeling biofilms. *cDynoMiCs* includes eucaryotic cell modeling processes with the addition of extracellular matrix and cellular mechanisms such as tight junctions and chemotaxis. Each cell is represented as a spherical particle, which has a particular biomass, and implements type and species-specific mechanisms to reproduce cellular physiology. Biochemically, particles can secrete or uptake chemicals that are diffused through the domain by executing reactions. Biomechanically, particles exhibit homogeneous and heterogeneous adhesion, and the formation of tight junctions. Particles model growth by increasing their biomass according to metabolic reactions and split into two particles once a maximum radius threshold is reached. They can also switch from one type of particle to another based on specific microenvironmental conditions and internal states. The simulation process interleaves biomechanical stress relaxation where the particles are moved in response to individual forces, along with the resolution of biochemical processes such as secretion, uptake, and diffusion by a differential equation solver. We assume that the solute fields are in a pseudo steady-state with respect to biomass growth [31].

Particle growth and division can cause particles to overlap, creating biomechanical stress. To resolve this problem a process called shoving is implemented. When the distance between two particles is less than a fixed threshold set by the particle size, a repulsive force is generated to push them apart, proportional to the overlap distance between the two particles. Then the relaxation process commences that iteratively moves each particle in response to its net force, then recalculates the forces due to the movement. The process terminates when only negligible forces remain, and the system has reached a pseudo steady state.

cDynoMiCs adds new functionality to the Java code of *iDynoMiCS* and extends the XML protocol, used to specify many different types of simulations. *iDynoMiCS* writes

plain-text XML files as output, and these may be processed using any number of software tools, such as Matlab and R. In addition to XML files, *iDynoMiCS* also writes files for POV-Ray that is used to render 3-D ray-traced images of the simulation. For the experiment to form the 1mm granule in Section 3.0.4, a 1.16 mm $\times$ 1.16 mm domain size was used. For all other experiments, a 508 μm $\times$ 508 μm domain size (2D) is used. A summary of the protocol parameter values can be found in Table 4.1.

Three solutes, glucose (S_g), acetate (S_a) and methane (S_m), exist within the reactor model. The distribution of these solutes is controlled by Equations 4.1, 4.2, and 4.3 respectively. The diffusion coefficients and reaction rates take different forms for each region depending upon the spatial distribution of acidogen biomass (B_a), methanogen biomass (B_m) and dead biomass (B_d) described in Equation 4.4. The effective diffusion coefficient is decreased within the granule compared with the liquid value in order to account for the increased mass transfer resistance. The diffusivity values used for the model (specified in Table 4.1) are taken from literature related to biofilm diffusivity studies [34,35]. The growth rate of acidogens is $\mu_a(S_g, S_a)$, defined in Equation 4.8, and the growth rate of methanogens is $\mu_m(S_a)$ defined in Equation 4.9.

$$\frac{\partial S_g}{\partial t} = B(x,y).D_g.\frac{\bigtriangledown^2 S_g}{\partial x \partial y} - \mu_a(S_g, S_a).\frac{B_a}{\alpha_{bg}} \tag{4.1}$$

$$\frac{\partial S_a}{\partial t} = B(x,y).D_a.\frac{\bigtriangledown^2 S_a}{\partial x \partial y} + \mu_a(S_g, S_a).\frac{\alpha_{ag}.B_a}{\alpha_{bg}} \tag{4.2}$$

$$\frac{\partial S_m}{\partial t} = B(x,y).D_m.\frac{\bigtriangledown^2 S_m}{\partial x \partial y} + \mu_m(S_a).\frac{B_m}{\alpha_{ba}} \tag{4.3}$$

where,

$$B(x,y) = \begin{cases} 1.0 & \text{if location } x,y \text{ contains no biomass} \\ \gamma & \text{if location } x,y \text{ contains biomass} \end{cases} \tag{4.4}$$

Table 4.1: Parameters used in model and their literature values

Parameter Summary				
Model parameter	Symbol	Value	Unit	References
Solutes				
Diffusion of Glucose in liquid	D_g	5.8x10^{-6}	m^2 /day	[32]
Diffusion of Acetate in liquid	D_a	1.05x10^{-4}	m^2 /day	[32]
Diffusion of methane in liquid	D_m	1.29x10^{-4}	m^2 /day	[33]
Biofilm Diffusivity	γ	30	%	[34, 35]
Acidogens				
Cell mass	B_a	300	fg	[36]
Division radius		3	μm	[37]
Maximum growth rate	$\hat{\mu_a}$	0.208	h^{-1}	[36], [38, 39]
Substrate saturation constant	Ks	0.26	g/L	[27, 39]
Product inhibition constant	Ki	0.1	g/L	[38, 39]
Biomass conversion rate	α_{bg}	0.3	$g_{biomass}/g_{glucose}$	[39, 40]
Substrate conversion rate	α_{ag}	0.82	$g_{acetate}/g_{glucose}$	[38–40]
Death delay		48	h	estimated
Death threshold		0.02	g/L	estimated
Methanogens				
Cell mass	B_m	1500	fg	[37]
Mass of EPS capsule		10	fg	[25, 41]
Division radius		3	μm	[37]
Maximum growth rate	$\hat{\mu_m}$	0.1	h^{-1}	[25, 41]
Substrate saturation constant	Ks	0.005	g/L	[25, 41]
Biomass conversion rate	α_{ba}	0.15	$g_{biomass}/g_{acetate}$	[25,27,42]
Substrate conversion rate	α_{ma}	0.26	$g_{methane}/g_{acetate}$	[25, 27]
Death delay		48	h	estimated
Death threshold		0.00001	g/L	estimated

$$\frac{\partial B_a}{\partial t} = \mu_a(S_g, S_a)B_a - die(B_a) \tag{4.5}$$

$$\frac{\partial B_m}{\partial t} = \mu_a.S_a.B_m - die(B_m) \tag{4.6}$$

$$\frac{\partial B_d}{\partial t} = die(B_a) + die(B_m) \tag{4.7}$$

Equations 4.5 and 4.6 describe acidogen and methanogen biomass changes as a function of local acetate and glucose concentration. Cell death due to lack of food is modeled using a discrete switching mechanism defined as the function $die(B_i)$ in the equations. Acidogen cells are converted to dead cells when the amount of glucose is below a threshold value (death threshold in Table 4.1) for a period of 48 hours. Similarly, the methanogen cells are converted to dead cells when the amount of glucose is below a threshold value (death threshold in Table 4.1) for a period of 48 hours. The rate of increase in dead cell mass is define in Equation 4.7. The parameter values for controlling cell death are estimated due to the lack of studies quantifying the response of acidogen and methanogen cells to nutritional stress.

$$\mu_a(S_g, S_a) = \hat{\mu}_a.\frac{S_g}{(K_{sg} + S_g)}.\frac{K_i}{(K_i + S_a)} \tag{4.8}$$

$$\mu_m(S_a) = \hat{\mu}_m\frac{S_a}{K_{sa} + S_a} \tag{4.9}$$

Acidogens grow by consuming glucose and producing acetate described by the monod-kinetic Equation 4.8, where $\hat{\mu}_a$ is the maximum growth rate for acidogens. Similarly, methanogen growth by consuming acetate and producing methane described by monod-kinetic Equation 4.9, where $\hat{\mu}_m$ is the maximum growth rate for mathanogens. Values for growth constants, such as biomass yield and substrate conversion rate, for both acidogens and methanogens were taken from literature and averaged. Thus, maximum growth rate

for acidogens was twice as high as that that of methanogens, see [3, 27, 39–44]. Biomass decay rate is not taken into account for both cell types, since decay for anaerobic type of growth is usually less or equal to 1% of specific growth rate and thus can be ignored [44]. Non-competitive product inhibition is considered for growth of acidogens [44], but not for the methanogens, assuming low inhibition of methanogenic growth by excess amount of acetate.

CHAPTER 5

DISCUSSION AND CONCLUSIONS

A model of anaerobic granulation from digestion of glucose to methane has been successfully implemented in an agent-based simulator framework, *cDynoMiCs*. Simulation studies incorporated modeling of both reactor and single agglomerate scale granule development. Utilized growth mechanisms for generalized glucose-consuming/acetate-producing bacteria and acetate-consuming/methane-producing bacteria resulted in a well-correlated kinetic patterns of substrate conversions and biomass growth (Figure 3.3). We were able to successfully qualitatively and quantitatively validate the architecture of the developed simulated anaerobic granule with the granule images and cell distribution from experimental literature studies (Figure 3.4)(Figure 3.5).

The described granulation model has direct applications for designs of experiments, to predict yields of methane gas from substrates of interest. One application of the model was successfully demonstrated in this paper via parameter scan algorithm, searching through different acidogens:methanogens cell ratios and glucose feed that is needed to start anaerobic system to achieve a desired (maximum) methane yield. By changing the parameters of microbial growth to fit bacteria of a specific interest (the bacteria one is targeting to explore in an AD experiment), researchers can apply this model to predict efficiencies of anaerobic digestion in a system. The tested parameter scan is directly applicable to the studies with low-strength feed streams to UASB reactors, such as AD of brewery wastewater (COD=100-800 mg/L) [45], some municipal and industrial wastewaters (COD=100-400 mg/L) [46, 47] and effluents from petroleum refineries (COD from 68 mg/L) [48]. Further development of the model will include a parameter search to investigate methane production from medium and high strength wastewaters.

The current model of anaerobic granulation and methane production from simple feed sources (glucose) can be expanded to accommodate microbial conversion of more substrates, such as a mixture and proteins and carbohydrates. This expansion will make it possible to study granulation and methane potential from a more realistic scenario of wastewater

feed, such as dairy and municipal wastewaters. A granulation model from a complex feed should result in a less stratified granule, due to the differential diffusions of the main feed components and a more complex patterns of microbial growth kinetics [18]. In addition, a model framework (cDynoMiCs) can be further modified to simulate detachment of excessive biomass from granular surface (simulating sheer stress described in the UASB reactor environment [4, 34, 49, 50]) and breakage of a granule into daughter clusters, that subsequently give rise to mature granules with a more complex morphology [18, 21, 51]). Another possible realm to expand development and application of current granulation model is to explore the mechanisms of enhancing anaerobic granulation, such as addition of positively charged ions and particles of polymers into the UASB system [52, 53]. The current model of the *de novo* anaerobic granulation and its immediate applications will aid future discoveries in the field of anaerobic digestion, which is regaining its value and popularity in sustainable energy.

REFERENCES

[1] Hulshoff Pol, L. W., Dolfing, J., Van Straten, K., De Zeeuw, W. J., and Lettinga, G., "Pelletization of anaerobic sludge in upflow anaerobic sludge bed reactors on sucrose-containing substrates," 1984.

[2] Zeeuw, W. D., *Acclimatization of anaerobic sludge for UASB-reactor start-up*, Ph.D. thesis, [Sl: sn], 1984.

[3] Kosaric, N., Blaszczyk, R., and Orphan, L., "Factors influencing formation and maintenance of granules in anaerobic sludge blanket reactors (UASBR)," *Water Science and Technology*, Vol. 22, No. 9, 1990, pp. 275–282.

[4] Tiwari, M. K., Guha, S., Harendranath, C. S., and Tripathi, S., "Influence of extrinsic factors on granulation in UASB reactor," *Applied microbiology and biotechnology*, Vol. 71, No. 2, 2006, pp. 145–154.

[5] Schmidt, J. E. E. and Ahring, B. K., "Extracellular polymers in granular sludge from different upflow anaerobic sludge blanket (UASB) reactors," *Applied Microbiology and Biotechnology*, Vol. 42, No. 2-3, 1994, pp. 457–462.

[6] Liu, Y., Xu, H.-L., Yang, S.-F., and Tay, J.-H., "Mechanisms and models for anaerobic granulation in upflow anaerobic sludge blanket reactor," *Water Research*, Vol. 37, No. 3, 2003, pp. 661–673.

[7] Kobayashi, T., Xu, K.-Q., and Chiku, H., "Release of extracellular polymeric substance and disintegration of anaerobic granular sludge under reduced sulfur compounds-rich conditions," *Energies*, Vol. 8, No. 8, 2015, pp. 7968–7985.

[8] Tay, J.-H., Xu, H.-L., and Teo, K.-C., "Molecular mechanism of granulation. I: H+ translocation-dehydration theory," *Journal of Environmental Engineering*, Vol. 126, No. 5, 2000, pp. 403–410.

[9] Teo, K.-C., Xu, H.-L., and Tay, J.-H., "Molecular mechanism of granulation. II: proton translocating activity," *Journal of Environmental Engineering*, Vol. 126, No. 5, 2000, pp. 411–418.

[10] Liu, X.-W., Sheng, G.-P., and Yu, H.-Q., "Physicochemical characteristics of microbial granules," *Biotechnology advances*, Vol. 27, No. 6, 2009, pp. 1061–1070.

[11] Batstone, D. J., Picioreanu, C., and Van Loosdrecht, M. C. M., "Multidimensional modelling to investigate interspecies hydrogen transfer in anaerobic biofilms," *Water research*, Vol. 40, No. 16, 2006, pp. 3099–3108.

[12] Lin, Y., Yin, J., Wang, J., and Tian, W., "Performance and microbial community in hybrid anaerobic baffled reactor-constructed wetland for nitrobenzene wastewater," *Bioresource technology*, Vol. 118, 2012, pp. 128–135.

[13] Tartakovsky, B. and Guiot, S. R., "Modeling and analysis of layered stationary anaerobic granular biofilms," *Biotechnology and bioengineering*, Vol. 54, No. 2, 1997, pp. 122–130.

[14] Arcand, Y., Chavarie, C., and Guiot, S. R., "Dynamic modelling of the population distribution in the anaerobic granular biofilm," *Water Science and Technology*, Vol. 30, No. 12, 1994, pp. 63–73.

[15] Shayegan, J., Ghavipanjeh, F., and Mehdizadeh1O, H., "Dynamic Modeling of Granular Sludge in UASB Reactors," *Iranian Journal of Chemical Engineering*, Vol. 2005, No. 1, pp. 53.

[16] Skiadas, I. V. and Ahring, B. K., "A new model for anaerobic processes of up-flow anaerobic sludge blanket reactors based on cellular automata," *Water science and technology*, Vol. 45, No. 10, 2002, pp. 87–92.

[17] Wimpenny, J. W. T. and Colasanti, R., "A unifying hypothesis for the structure of microbial biofilms based on cellular automaton models," *FEMS Microbiology Ecology*, Vol. 22, No. 1, 1997, pp. 1–16.

[18] Rocheleau, S., Greer, C. W., Lawrence, J. R., Cantin, C., Laramée, L., and Guiot, S. R., "Differentiation of Methanosaeta concilii andMethanosarcina barkeri in Anaerobic Mesophilic Granular Sludge by Fluorescent In Situ Hybridization and Confocal Scanning Laser Microscopy," *Applied and environmental microbiology*, Vol. 65, No. 5, 1999, pp. 2222–2229.

[19] Sekiguchi, Y., Kamagata, Y., Nakamura, K., Ohashi, A., and Harada, H., "Fluorescence in situ hybridization using 16S rRNA-targeted oligonucleotides reveals localization of methanogens and selected uncultured bacteria in mesophilic and thermophilic sludge granules," *Applied and Environmental Microbiology*, Vol. 65, No. 3, 1999, pp. 1280–1288.

[20] Fang, H. H., "Microbial distribution in UASB granules and its resulting effects," *Water Science and Technology*, Vol. 42, No. 12, 2000, pp. 201–208.

[21] Batstone, D. J., Keller, J., and Blackall, L. L., "The influence of substrate kinetics on the microbial community structure in granular anaerobic biomass," *Water Research*, Vol. 38, No. 6, 2004, pp. 1390–1404.

[22] Picioreanu, C., Batstone, D. J., and Van Loosdrecht, M. C. M., "Multidimensional modelling of anaerobic granules," *Water Science and Technology*, Vol. 52, No. 1-2, 2005, pp. 501–507.

[23] Batstone, D. J., Keller, J., Angelidaki, I., Kalyuzhnyi, S. V., Pavlostathis, S. G., Rozzi, A., Sanders, W. T. M., Siegrist, H., and Vavilin, V. A., "The IWA anaerobic digestion model no 1 (ADM1)," *Water Science and Technology*, Vol. 45, No. 10, 2002, pp. 65–73.

[24] Batstone, D. J., Puyol, D., Flores-Alsina, X., and Rodr'iguez, J., "Mathematical modelling of anaerobic digestion processes: applications and future needs," *Reviews in Environmental Science and Bio/Technology*, Vol. 14, No. 4, 2015, pp. 595–613.

[25] Nishio, N., Kuroda, K., Nagai, S., and Others, "Methanogenesis of glucose by defined thermophilic coculture of Clostridium thermoaceticum and Methanosarcina sp." *Journal of fermentation and bioengineering*, Vol. 70, No. 6, 1990, pp. 398–403.

[26] Kalyuzhnyy, S. V., Gachok, V. P., Sklyar, V. I., and Varfolomeyev, S. D., "Kinetic investigation and mathematical modeling of methanogenesis of glucose," *Applied biochemistry and biotechnology*, Vol. 28, No. 1, 1991, pp. 183–195.

[27] Kalyuzhnyi, S. V. and Davlyatshina, M. A., "Batch anaerobic digestion of glucose and its mathematical modeling. I. Kinetic investigations," *Bioresource Technology*, Vol. 59, No. 1, 1997, pp. 73–80.

[28] Fang, C., Boe, K., and Angelidaki, I., "Anaerobic co-digestion of by-products from sugar production with cow manure," *Water Research*, Vol. 45, No. 11, 2011, pp. 3473–3480.

[29] Britz, T. J., Van Schalkwyk, C., and Roos, P., "Development of a method to enhance granulation in a laboratory batch system," *Water SA*, Vol. 28, No. 1, 2002, pp. 49–54.

[30] Baker, Q. B., Podgorski, G. J., Johnson, C. D., Vargis, E., and Flann, N. S., "Bridging the multiscale gap: Identifying cellular parameters from multicellular data," *Computational Intelligence in Bioinformatics and Computational Biology (CIBCB), 2015 IEEE Conference on*, IEEE, Aug. 2015, pp. 1–7.

[31] Lardon, L. A., Merkey, B. V., Martins, S., Dötsch, A., Picioreanu, C., Kreft, J.-U. U., and Smets, B. F., "iDynoMiCS: next-generation individual-based modelling of biofilms." *Environmental microbiology*, Vol. 13, No. 9, Sept. 2011, pp. 2416–2434.

[32] Hobbie, R. and Roth, B. J., *Intermediate physics for medicine and biology*, Springer Science & Business Media, 2007.

[33] Haynes, W. M., "the CRC Handbook of Chemistry and Physics 93RD Edition, 2012," *Chemical Rubber Company*.

[34] Lens, P. N. L., Gastesi, R., Vergeldt, F., van Aelst, A. C., Pisabarro, A. G., and Van As, H., "Diffusional properties of methanogenic granular sludge: 1H NMR characterization," *Applied and environmental microbiology*, Vol. 69, No. 11, 2003, pp. 6644–6649.

[35] Stewart, P. S., "Diffusion in biofilms," *Journal of bacteriology*, Vol. 185, No. 5, 2003, pp. 1485–1491.

[36] Kubitschek, H. E., "Cell volume increase in Escherichia coli after shifts to richer media." *Journal of bacteriology*, Vol. 172, No. 1, 1990, pp. 94–101.

[37] Sowers, K. R., Baron, S. F., and Ferry, J. G., "Methanosarcina acetivorans sp. nov., an acetotrophic methane-producing bacterium isolated from marine sediments," *Applied and Environmental Microbiology*, Vol. 47, No. 5, 1984, pp. 971–978.

[38] Gavala, H. N., Angelidaki, I., and Ahring, B. K., "Kinetics and modeling of anaerobic digestion process," *Biomethanation I*, Springer, 2003, pp. 57–93.

[39] Ibba, M. and Fynn, G. H., "Two stage methanogenesis of glucose byAcetogenium kivui and acetoclastic methanogenic Sp." *Biotechnology letters*, Vol. 13, No. 9, 1991, pp. 671–676.

[40] Bhunia, P. and Ghangrekar, M. M., "Analysis, evaluation, and optimization of kinetic parameters for performance appraisal and design of UASB reactors," *Bioresource Technology*, Vol. 99, No. 7, 2008, pp. 2132–2140.

[41] Moletta, R., Verrier, D., and Albagnac, G., "Dynamic modelling of anaerobic digestion," *Water Research*, Vol. 20, No. 4, 1986, pp. 427–434.

[42] Yang, S.-T. and Okos, M. R., "Kinetic study and mathematical modeling of methanogenesis of acetate using pure cultures of methanogens," *Biotechnology and bioengineering*, Vol. 30, No. 5, 1987, pp. 661–667.

[43] SiÑEriz, F. and Pirt, S. J., "Methane production from glucose by a mixed culture of bacteria in the chemostat: the role of Citrobacter," *Microbiology*, Vol. 101, No. 1, 1977, pp. 57–64.

[44] Gavala, H. N., Angelidaki, I., and Ahring, B. K., *Kinetics and Modeling of Anaerobic Digestion Process*, Springer Berlin Heidelberg, Berlin, Heidelberg, 2003, pp. 57–93.

[45] Kato, M. T., Field, J. A., and Lettinga, G., "The anaerobic treatment of low strength wastewaters in UASB and EGSB reactors," *Water Science and Technology*, Vol. 36, No. 6-7, 1997, pp. 375–382.

[46] Álvarez, J. A., Armstrong, E., Gómez, M., and Soto, M., "Anaerobic treatment of low-strength municipal wastewater by a two-stage pilot plant under psychrophilic conditions," *Bioresource Technology*, Vol. 99, No. 15, 2008, pp. 7051–7062.

[47] Kumar, A., Yadav, A. K., Sreekrishnan, T. R., Satya, S., and Kaushik, C. P., "Treatment of low strength industrial cluster wastewater by anaerobic hybrid reactor," *Bioresource Technology*, Vol. 99, No. 8, 2008, pp. 3123–3129.

[48] Diya'uddeen, B. H., Daud, W. M., and Aziz, A. R. A., "Treatment technologies for petroleum refinery effluents: A review," *Process Safety and Environmental Protection*, Vol. 89, No. 2, 2011, pp. 95–105.

[49] Pol, L. H., de Castro Lopes, S. I., Lettinga, G., and Lens, P. N. L., "Anaerobic sludge granulation," *Water Research*, Vol. 38, No. 6, 2004, pp. 1376–1389.

[50] Alphenaar, P. A., Visser, A., and Lettinga, G., "The effect of liquid upward velocity and hydraulic retention time on granulation in UASB reactors treating wastewater with a high sulphate content," *Bioresource Technology*, Vol. 43, No. 3, 1993, pp. 249–258.

[51] MacLeod, F., Guiot, S., and Costerton, J., "Layered structure of bacterial aggregates produced in an upflow anaerobic sludge bed and filter reactor." *Applied and Environmental Microbiology*, Vol. 56, No. 6, 1990, pp. 1598–1607.

[52] Mahoney, E. M., Varangu, L. K., Cairns, W. L., Kosaric, N., and Murray, R. G., "The effect of calcium on microbial aggregation during UASB reactor start-up," *Water Science and Technology*, Vol. 19, No. 1-2, 1987, pp. 249–260.

[53] Show, K.-Y., Wang, Y., Foong, S.-F., and Tay, J.-H., "Accelerated start-up and enhanced granulation in upflow anaerobic sludge blanket reactors," *Water Research*, Vol. 38, No. 9, 2004, pp. 2293–2304.

APPENDICES

Appendix A

Protocol file for the model

A.1 Description

This xml document function as the definition of the model and as the input to the simulation framework.

A.2 Protocol file

```
1
2 <?xml version="1.0" encoding="UTF-8" standalone="no"?><!--
3
4 ##########################################################################
5  iDynoMiCS: individual-based Dynamics of Microbial Communities Simulator
6 ##########################################################################
7
8 --><idynomics>
9     <!--
          ##########################################################################
10        SIMULATOR SECTION
11    ##########################################################################
          -->
12    <simulator>
13        <param name="restartPreviousRun">false</param>
14        <param name="randomSeed">12</param>
15        <param name="outputPeriod" unit="hour">325</param>
16        <timeStep>
17            <param name="adaptive">false</param>
18            <param name="timeStepIni" unit="hour">1</param>
19            <param name="timeStepMin" unit="hour">1</param>
20            <param name="timeStepMax" unit="hour">1</param>
21            <param name="endOfSimulation" unit="hour">650</param>
```

```
22      </timeStep>
23      <!-- The AGENTTIMESTEP which should always be EQUAL or LOWER than
            the global time step -->
24      <param name="agentTimeStep" unit="hour">1</param>
25  </simulator>
26  <!--
        ##########################################################################

        INPUT SECTION
    ##########################################################################
        -->
29  <input>
30      <param name="useAgentFile">false</param>
31      <param name="inputAgentFileURL">agent_State(last).xml</param>
32      <param name="useBulkFile">false</param>
33      <param name="inputBulkFileURL">env_Sum(last).xml</param>
34  </input>
35  <!--
        ##########################################################################

        SOLUTES AND BIOMASS TYPES SECTION
    ##########################################################################
        -->
38  <solute domain="Granule" name="Attract">
39      <param name="diffusivity" unit="m2.day-1">1e-1</param>
40      <param name="airDiffusivity" unit="m2.day-1">1e-1</param>
41      <param name="concentration" unit="g.L-1">0</param>
42      <param name="writeOutput">true</param>
43  </solute>
44  <solute domain="Granule" name="pressure">
45      <param name="diffusivity" unit="m2.day-1">1</param>
46      <!--<param name="concentration" unit="g.L-1">0</param>-->
47  </solute>
48  <solute domain="Granule" name="Glucose">
49      <param name="diffusivity" unit="m2.day-1">5.8e-6</param>
```

```
50      <!—higher in biomass than in liquid—>
51      <param name="airDiffusivity" unit="m2.day-1">5.8e-6</param>
52      <param name="writeOutput">true</param>
53      <!—<param name="concentration" unit="g.L-1">0</param>—>
54    </solute>
55    <solute domain="Granule" name="Acetate">
56      <param name="diffusivity" unit="m2.day-1">1.05e-4</param>
57      <!—higher in biomass than in liquid—>
58
59      <param name="writeOutput">true</param>
60      <!— <param name="concentration" unit="g.L-1">0</param>—>
61    </solute>
62    <solute domain="Granule" name="Methane">
63      <param name="diffusivity" unit="m2.day-1">1.29e-4</param>
64       <param name="airDiffusivity" unit="m2.day-1">1.29e-4</param>
65      <!—higher in biomass than in liquid—>
66
67      <param name="writeOutput">true</param>
68      <!—<param name="concentration" unit="g.L-1">0</param>—>
69    </solute>
70    <particle name="biomass">
71      <param name="density" unit="g.L-1">150</param>
72      <!—<param name="concentration" unit="g.L-1">0</param>—>
73    </particle>
74    <particle name="inert">
75      <param name="density" unit="g.L-1">150</param>
76      <!—<param name="concentration" unit="g.L-1">0</param>—>
77    </particle>
78    <particle name="capsule">
79      <param name="density" unit="g.L-1">78</param>
80      <!—<param name="concentration" unit="g.L-1">0</param>—>
81    </particle>
82    <!—
        ##########################################################################
```

```
83        WORLD SECTION
84    ################################################################################
          -->
85    <world>
86        <bulk name="MyTank">
87            <param name="isConstant">false</param>
88            <!--<param name= "D" unit= "h-1">0.05</param>-->
89            <solute name="Glucose">
90                <param name="isConstant">false</param>
91                <param name="Sbulk" unit="g.L-1">0.4</param>
92 <!--               <param name="Sin" unit="g.L-1">0</param>
93                <param name="Spulse" unit="g.L-1">0.4</param>
94                <param name="pulseRate" unit="h-1">0.005</param -->
95            </solute>
96            <solute name="Attract">
97                <param name="isConstant">true</param>
98                <param name="Sbulk" unit="g.L-1">0</param>
99                <param name="Sin" unit="g.L-1">0</param>
100               <param name="Spulse" unit="g.L-1">0</param>
101               <param name="pulseRate" unit="h-1">0</param>
102           </solute>
103           <solute name="Methane">
104               <param name="isConstant">true</param>
105               <param name="Sbulk" unit="g.L-1">0</param>
106               <param name="Sin" unit="g.L-1">0</param>
107               <param name="Spulse" unit="g.L-1">0</param>
108               <param name="pulseRate" unit="h-1">0</param>
109           </solute>
110           <solute name="Acetate">
111               <param name="isConstant">true</param>
112               <param name="Sbulk" unit="g.L-1">0</param>
113               <param name="Sin" unit="g.L-1">0</param>
114               <param name="Spulse" unit="g.L-1">0</param>
115               <param name="pulseRate" unit="h-1">0</param>
116           </solute>
```

```
117         </bulk>
118         <computationDomain name="Granule">
119             <grid nDim="2" nI="127" nJ="127" nK="1" />
120             <param name="resolution" unit="um">4</param>
121             <param name="boundaryLayer" unit="um">0</param>
122             <param name="biofilmDiffusivity">0.3</param>
123             <param name="specificArea" unit="m2.m-3">80</param>
124             <boundaryCondition class="BoundaryBulk" name="y0z">
125                 <param name="activeForSolute">yes</param>
126                 <param detail="Glucose" name="isPermeableTo">true</param>
127                 <!-- <param detail="Methane" name="isPermeableTo">true</param>
                        -->
128                 <param name="bulk">MyTank</param>
129                 <shape class="Planar">
130                     <param name="pointIn" x="-1" y="0" z="0" />
131                     <param name="vectorOut" x="-1" y="0" z="0" />
132                 </shape>
133             </boundaryCondition>
134             <boundaryCondition class="BoundaryBulk" name="yNz">
135 <param name="activeForSolute">yes</param>
136                 <param detail="Glucose" name="isPermeableTo">true</param>
137             <!--  <param detail="Methane" name="isPermeableTo">true</param>
                    -->
138                 <param name="bulk">MyTank</param>
139                 <shape class="Planar">
140                     <param name="pointIn" x="127" y="0" z="0" />
141                     <param name="vectorOut" x="1" y="0" z="0" />
142                 </shape>
143             </boundaryCondition>
144             <boundaryCondition class="BoundaryBulk" name="x0z">
145 <param name="activeForSolute">yes</param>
146                 <param detail="Glucose" name="isPermeableTo">true</param>
147             <!--  <param detail="Methane" name="isPermeableTo">true</param>
                    -->
148                 <param name="bulk">MyTank</param>
```

```
149             <shape class="Planar">
150                 <param name="pointIn" x="0" y="-1" z="0"/>
151                 <param name="vectorOut" x="0" y="-1" z="0"/>
152             </shape>
153         </boundaryCondition>
154         <boundaryCondition class="BoundaryBulk" name="xNz">
155 <param name="activeForSolute">yes</param>
156             <param detail="Glucose" name="isPermeableTo">true</param>
157         <!--  <param detail="Methane" name="isPermeableTo">true</param>
                -->
158             <param name="bulk">MyTank</param>
159             <shape class="Planar">
160                 <param name="pointIn" x="0" y="127" z="0"/>
161                 <param name="vectorOut" x="0" y="1" z="0"/>
162             </shape>
163         </boundaryCondition>
164         <boundaryCondition class="BoundaryZeroFlux" name="x0y">
165             <shape class="Planar">
166                 <param name="pointIn" x="0" y="0" z="-1"/>
167                 <param name="vectorOut" x="0" y="0" z="-1"/>
168             </shape>
169         </boundaryCondition>
170         <boundaryCondition class="BoundaryZeroFlux" name="x0y">
171
172             <shape class="Planar">
173                 <param name="pointIn" x="0" y="0" z="1"/>
174                 <param name="vectorOut" x="0" y="0" z="1"/>
175             </shape>
176         </boundaryCondition>
177     </computationDomain>
178 </world>
179 <!--
        ##########################################################################

180     REACTION SECTION
```

```
181  ##########################################################################
         -->
182  <reaction catalyzedBy="biomass" class="ReactionFactor" name="
         GlucoseDegradation">
183      <param name="muMax" unit="h-1">0.208</param>
184      <kineticFactor class="MonodKinetic" solute="Glucose">
185          <param name="Ks" unit="g.L-1">0.26</param>
186      </kineticFactor>
187      <kineticFactor class="SimpleInhibition" solute="Acetate">
188          <param name="Ki" unit="g.L-1">0.1</param>
189      </kineticFactor>
190      <yield>
191          <param name="Glucose" unit="g.g-1">-1</param>
192          <param name="biomass" unit="g.g-1">0.3</param>
193          <param name="Acetate" unit="g.g-1">0.82</param>
194      </yield>
195  </reaction>
196  <reaction catalyzedBy="biomass" class="ReactionFactor" name="
         AcetateDegradation">
197      <param name="muMax" unit="h-1">0.1</param>
198      <kineticFactor class="MonodKinetic" solute="Acetate">
199          <!--will be inhibited later by NH3!-->
200          <param name="Ks" unit="g.L-1">0.005</param>
201      </kineticFactor>
202      <yield>
203          <param name="Acetate" unit="g.g-1">-1</param>
204          <param name="biomass" unit="g.g-1">0.15</param>
205          <param name="Methane" unit="g.g-1">0.26</param>
206          <param name="capsule" unit="g.g-1">0.08</param>
207      </yield>
208  </reaction>
209  <reaction catalyzedBy="biomass" class="ReactionFactor" name="
         AttractSecretion">
210      <param name="muMax" unit="hour-1">0.03</param>
211      <kineticFactor class="FirstOrderKinetic"/>
```

```
212         <yield>
213             <param name="Attract" unit="g.g-1">0.05</param>
214         </yield>
215     </reaction>
216     <reaction catalyzedBy="biomass" class="ReactionFactor" name="Death">
217         <param name="muMax" unit="hour-1">10</param>
218         <kineticFactor class="FirstOrderKinetic"/>
219         <yield>
220             <param name="biomass" unit="g.g-1">-10</param>
221         </yield>
222     </reaction>
223     <!--
        ########################################################################

224         SOLVER SECTION
225     ########################################################################
        -->
226     <solver class="SolverSimple" domain="Granule" name="solutes">
227         <param name="active">true</param>
228         <param name="preStep">40</param>
229         <param name="postStep">40</param>
230         <param name="coarseStep">1500</param>
231         <param name="nCycles">5</param>
232         <reaction name="GlucoseDegradation"/>
233         <reaction name="AcetateDegradation"/>
234         <reaction name="AttractSecretion"/>
235         <reaction name="Death"/>
236     </solver>
237     <!-- <solver class="Solver_pressure" name="pressure" domain="Granule"><
        param name="active">true</param></solver> -->
238     <!--
        ########################################################################

239         AGENT GRID SECTION
```

```
240 ##########################################################################
        -->
241 <agentGrid>
242     <param name="computationDomain">Granule</param>
243     <param name="resolution" unit="um">4</param>
244     <!-- <detachment class="DS_Biomass"><param name="kDet" unit="fg.um
            -4.hour-1.">2e-4</param><param name="maxTh" unit="um">300</param
            ></detachment><param name="sloughDetachedBiomass">true</param>
            -->
245     <param name="shovingMaxNodes">2e6</param>
246     <param name="shovingFraction">1</param>
247     <param name="shovingMaxIter">50</param>
248     <param name="shovingMutual">true</param>
249 </agentGrid>
250 <!--
        ##########################################################################

        SPECIES SECTION
252 ##########################################################################
        -->
253
254 <!--
        ##########################################################################

        GDyingA SECTION
256 ##########################################################################
        -->
257 <species class="Yeast" name="GDyingA">
258     <particle name="biomass">
259         <param name="mass" unit="fg">300</param>
260     </particle>
261     <particle name="inert">
262         <param name="mass" unit="fg">0</param>
263     </particle>
264     <param name="color">black</param>
```

```
265         <param name="computationDomain">Granule</param>
266         <param name="divRadius" unit="um">10000</param>
267         <param name="deathRadius" unit="um">0</param>
268         <param name="shoveFactor" unit="um">1</param>
269         <param name="shoveLimit" unit="um">0</param>
270         <param name="agitationCV">0.2</param>
271         <!--<reaction name="Death" status="active" />-->
272         <entryConditions>
273             <entryCondition name="Glucose" type="solute">
274                 <param name="fromSpecies">Acidogen</param>
275                 <param name="switch">lessThan</param>
276                 <param name="concentration" unit="g.L-1">0.02</param>
277             </entryCondition>
278         </entryConditions>
279         <adhesions>
280             <adhesion strength="1" withSpecies="GDyingA"/>
281             <adhesion strength="1" withSpecies="Acidogen"/>
282             <adhesion strength="1" withSpecies="Methanogen"/>
283         </adhesions>
284         <tightJunctions>
285             <tightJunction stiffness="0" withSpecies="GDyingA"/>
286             <tightJunction stiffness="0" withSpecies="Acidogen"/>
287             <tightJunction stiffness="0" withSpecies="Methanogen"/>
288         </tightJunctions>
289     </species>
290     <!--
            ##########################################################################

291         Acidogen
292     ##########################################################################
            -->
293     <species class="Yeast" name="Acidogen">
294         <particle name="biomass">
295             <param name="mass" unit="fg">300</param>
296         </particle>
```

```
297         <particle name="inert">
298             <param name="mass" unit="fg">0</param>
299         </particle>
300         <param name="color">green</param>
301         <param name="computationDomain">Granule</param>
302         <param name="divRadius" unit="um">2</param>
303         <param name="deathRadius" unit="um">0</param>
304         <param name="shoveFactor" unit="um">1</param>
305         <param name="shoveLimit" unit="um">0.0</param>
306
307         <!-- <param name="divRadiusCV">1</param><param name="deathRadiusCV">
                1</param><param name="babyMassFracCV">1</param> -->
308         <reaction name="GlucoseDegradation" status="active"/>
309         <chemotaxis>
310             <chemotactic strength="5" withSolute="Attract"/>
311         </chemotaxis>
312         <entryConditions>
313             <!-- <entryCondition name="Glucose" type="solute"><param name="
                    fromSpecies">GDyingA</param><param name="switch">greaterThan<
                    /param><param name="concentration" unit="g.L-1">0.1</param></
                    entryCondition> -->
314         </entryConditions>
315         <tightJunctions>
316             <tightJunction stiffness="0" withSpecies="Acidogen"/>
317             <tightJunction stiffness="0" withSpecies="Methanogen"/>
318             <tightJunction stiffness="0" withSpecies="GdyingA"/>
319         </tightJunctions>
320         <switchingLags>
321             <switchingLag toSpecies="GDyingA" unit="hour" value="48"/>
322         </switchingLags>
323         <adhesions>
324             <adhesion strength="2" withSpecies="Methanogen"/>
325             <adhesion strength="1" withSpecies="Acidogen"/>
326             <adhesion strength="0" withSpecies="GdyingA"/>
327         </adhesions>
```

```
328         <initArea number="100">
329             <param name="birthday" unit="hour">0</param>
330             <coordinates x="245" y="245" z="0"/>
331             <coordinates x="250" y="250" z="0"/>
332         </initArea>
333     </species>
334     <!--
            ##########################################################################

335         Methanogen
336     ##########################################################################
            -->
337     <species class="Yeast" name="Methanogen">
338         <particle name="biomass">
339             <param name="mass" unit="fg">1500</param>
340         </particle>
341         <particle name="inert">
342             <param name="mass" unit="fg">10</param>
343         </particle>
344         <param name="color">red</param>
345         <param name="computationDomain">Granule</param>
346         <param name="divRadius" unit="um">3</param>
347         <param name="deathRadius" unit="um">0.001</param>
348         <param name="shoveFactor" unit="um">0.65</param>
349         <param name="shoveLimit" unit="um">0</param>
350
351         <!--<param name="divRadiusCV">1</param><param name="deathRadiusCV">1
                </param><param name="babyMassFracCV">1</param>  -->
352         <param name="epsMax">0.1</param>
353         <param name="kHyd" unit="hr-1">0.07</param>
354         <reaction name="AcetateDegradation" status="active"/>
355         <reaction name="AttractSecretion" status="active"/>
356         <entryConditions>
357             <!-- <entryCondition name="Acetate" type="solute"><param name="
                    fromSpecies">GDyingM</param><param name="switch">greaterThan<
```

```
            /param><param name="concentration" unit="g.L-1">0.01</param><
            /entryCondition> -->
358     </entryConditions>
359     <tightJunctions>
360         <tightJunction stiffness="0" withSpecies="Methanogen"/>
361         <tightJunction stiffness="0" withSpecies="Acidogen"/>
362     </tightJunctions>
363     <switchingLags>
364         <switchingLag toSpecies="GDyingM" unit="hour" value="48"/>
365     </switchingLags>
366     <adhesions>
367         <adhesion strength="0" withSpecies="Methanogen"/>
368         <adhesion strength="2" withSpecies="Acidogen"/>
369                     <adhesion strength="0" withSpecies="GdyingA"/>
370     </adhesions>
371     <initArea number="110">
372         <param name="birthday" unit="hour">0</param>
373         <coordinates x="245" y="245" z="0"/>
374         <coordinates x="250" y="250" z="0"/>
375     </initArea>
376 </species>
377
378 <!--
        ##########################################################################

379     GDyingM
380 ##########################################################################
        -->
381 <species class="Yeast" name="GDyingM">
382     <particle name="biomass">
383         <param name="mass" unit="fg">1500</param>
384     </particle>
385     <particle name="inert">
386         <param name="mass" unit="fg">0</param>
387     </particle>
```

```
388         <param name="color">black</param>
389         <param name="computationDomain">Granule</param>
390         <param name="divRadius" unit="um">10000</param>
391         <param name="deathRadius" unit="um">0</param>
392         <param name="shoveFactor" unit="um">1</param>
393         <param name="shoveLimit" unit="um">0</param>
394         <!-- <param name="divRadiusCV">1</param><param name="deathRadiusCV">
                1</param><param name="babyMassFracCV">1</param> -->
395         <!--<reaction name="Death" status="active" />-->
396         <entryConditions>
397             <entryCondition name="Acetate" type="solute">
398                 <param name="fromSpecies">Methanogen</param>
399                 <param name="switch">lessThan</param>
400                 <param name="concentration" unit="g.L-1">0.00001</param>
401             </entryCondition>
402         </entryConditions>
403     </species>
404 </idynomics>
```